

## Modelling of argon/dust pulsed plasma

I. B. Denysenko<sup>1,2,3</sup>, I. Stefanović<sup>4</sup>, M. Mikikian<sup>2</sup>, E. Kovacevic<sup>2</sup>, J. Berndt<sup>2</sup>

<sup>1</sup>*School of Physics and Technology, V. N. Karazin Kharkiv National University, Ukraine*

<sup>2</sup>*GREMI, UMR 7344 CNRS/Université d'Orléans, F-45067 Orléans, France*

<sup>3</sup>*Le Studium, Loire Valley Institute for Advanced Studies, Orléans & Tours, France*

<sup>4</sup>*Institute of Technical Sciences, Serbian Academy of Sciences and Arts, Belgrade, Serbia*

We analyze how properties of an argon/dust pulsed plasma depend on the shape of the electron energy probability function (EEPF) and the pulsing frequency. The study is carried out using a spatially averaged model, which assumes that the plasma has  $R = 15$  cm radius and  $L = 7$  cm height and consists of electrons with density  $n_e$ , singly charged positive ions ( $\text{Ar}^+$ ) with density  $n_i$ , dust particles with density  $n_d = 3.0 \times 10^7 \text{ cm}^{-3}$ , radius  $a_d = 50 \text{ nm}$  and negative charge  $eZ_d$  ( $e$  is the elementary charge), ground-state argon atoms ( $\text{Ar}_0$ ) with density  $n_a$ , metastable argon atoms ( $\text{Ar}_m$ ) with density  $n_m$ , argon atoms in the resonance 4s states ( $^3\text{P}_1$  and  $^1\text{P}_1$ ) as well as argon atoms in 4p states. The neutral gas pressure  $P$  is 10 Pa, and the EEPF is described as

$F(\varepsilon) = A_1 \exp(-A_2 \varepsilon^{x_F})$ , where  $\varepsilon$  is the electron energy and  $x_F$  takes different values according to the shape of EEPF:  $x_F = 1$  and  $x_F = 2$  for Maxwellian and Druyvesteyn electron energy distributions, respectively. The coefficients  $A_1$  and  $A_2$  are functions of  $x_F$  and the average electron energy [1]. We also assume that ions and dust particles are at gas temperature  $T_g$  and ions have Maxwellian distribution.

The density of a species  $Y$  (electrons and argon atoms in excited states) as a function of time  $t$  is found from the following balance equation

$$\frac{\partial n^{(Y)}}{\partial t} = \sum_i R_{G,i}^{(Y)} - \sum_i R_{L,i}^{(Y)}, \quad (1)$$

where  $R_{G,i}^{(Y)}$  and  $R_{L,i}^{(Y)}$  are, respectively, the rates for reactions of the various generation and loss processes of the species  $Y$ . We assume that in both pure argon and dusty pulsed plasmas, electrons are generated in collisions of electrons with argon atoms in the ground and excited states (4p and 4s states), as well as in metastable–metastable collisions. In the dusty plasma, we assume that electrons can be additionally produced at interaction of excited argon atoms with acetylene molecules [2]. It is assumed that acetylene molecules are present with the very low density ( $\sim 10^{11} \text{ cm}^{-3}$ ) in the pulsed dusty plasma since the experimental procedure of making the dust plasma involves the use of acetylene as a precursor [2]. Electrons and ions are lost from the discharge because of their diffusion to the walls and by deposition on dust particles. The

plasma is assumed to be quasineutral ( $n_i - n_e + n_d Z_d = 0$ ). The effective electron temperature,  $T_{\text{eff}} = (2/3e) \int_0^\infty \varepsilon F(\varepsilon) \sqrt{\varepsilon} d\varepsilon$ , as a function of time was found from the power balance equation [3], assuming that the effective electron temperature cannot be smaller than the afterglow temperature  $T_{\text{aft}}$ , i.e. after its decay to reach  $T_{\text{aft}}$ ,  $T_{\text{eff}}$  becomes time-independent. Here,  $T_{\text{aft}} = 0.15$  eV and  $T_{\text{aft}} = 0.1$  eV for the dust-free and dusty cases, respectively. It is also assumed that the absorbed power is modulated by an ideal rectangular waveform

$$P_{\text{abs}} = \begin{cases} P_{\text{max}} & \text{for } (k-1)\tau \leq t < (k-1)\tau + \eta\tau, \\ 0 & \text{for } (k-1)\tau + \eta\tau \leq t < k\tau, \end{cases} \quad (2)$$

where  $\tau$  is the full cycle period,  $\eta$  is the duty cycle, and  $k$  is a positive integer.  $P = P_{\text{max}}$  for the on-period and  $P = 0$  for the off-period.

The dust charge as a function of time is found from the following equation:

$$\frac{\partial Z_d}{\partial t} = K_i^d n_i - K_e^d n_e, \quad (3)$$

where  $K_i^d$  and  $K_e^d$  are the rates describing collection of ions and electrons by dust particles, respectively. More details on the model equations and the reaction rates can be found in [3].

Using the model, we calculated plasma properties ( $n_e$ ,  $n_m$ ,  $T_{\text{eff}}$  and  $Z_d$ ) as a function of time in dust-free and dusty plasmas for the conditions typical to experiments on pure argon and argon/dust pulsed plasmas [2]. Fig. 1 illustrates the temporal behavior of the line-of-sight averaged electron density [(a) and (c)] and Ar\* 1s<sub>5</sub> metastable density [(b) and (d)] measured at the mid-plane between electrodes and the corresponding simulation results. The results of calculations are in a good qualitative agreement with the experimental data.

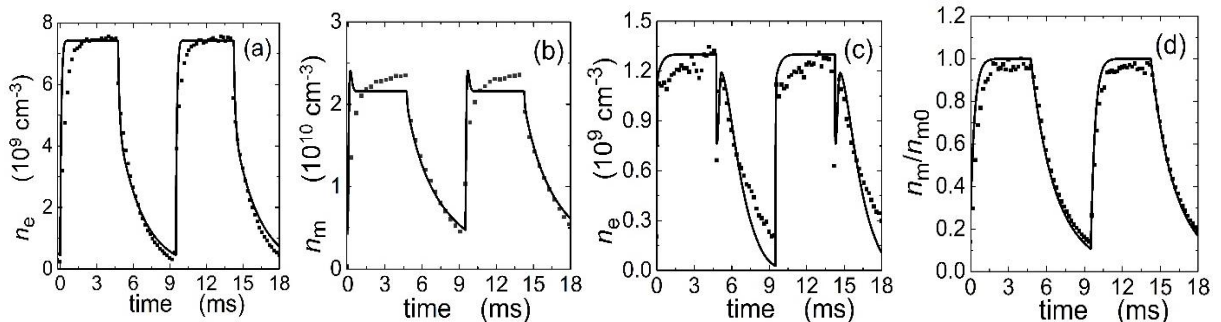


Fig. 1. Electron [(a) and (c)] and metastable [(b) and (d)] densities as a function of time in a pulsed plasma for the dust-free [(a) and (b)] and dusty [(c) and (d)] cases. Solid lines — model; black squares — experiment [2]. Zero time indicates the beginning of the on-period. The off-period (afterglow phase) starts at 4.75 ms and ends at 9.5 ms.  $n_{m0} = 9.64 \times 10^{10} \text{ cm}^{-3}$  and  $n_{m0} = 1.75 \times 10^{11} \text{ cm}^{-3}$  for the model and experiment, respectively. Here,  $x_F = 2$ .

The simulations were carried out for different shapes of the EEPF (Fig. 2). It is found that with increasing  $x_F$ , the EEPF becomes more convex and the effective electron temperature in the on-period increases [Fig. 2(a)]. As a result, the metastable density becomes larger [Fig. 2(b)]. The increase of  $n_m$  is accompanied by increasing the electron density in the off-period [Fig. 2(c)]. At the end of the on-period, the calculated metastable densities for  $x_F = 1$  and  $x_F = 1.5$  [Fig. 2(b)] are much smaller than the measured one ( $1.75 \times 10^{11} \text{ cm}^{-3}$ ). Moreover, the time-dependence for  $n_e$  in the case  $x_F = 1$  [Fig. 2(c)] differs essentially from the experimental data [Fig. 1(c)]. Thus, the results of theory and experiment agree better if the EEPF has a Druyvesteyn shape instead of a Maxwellian one.

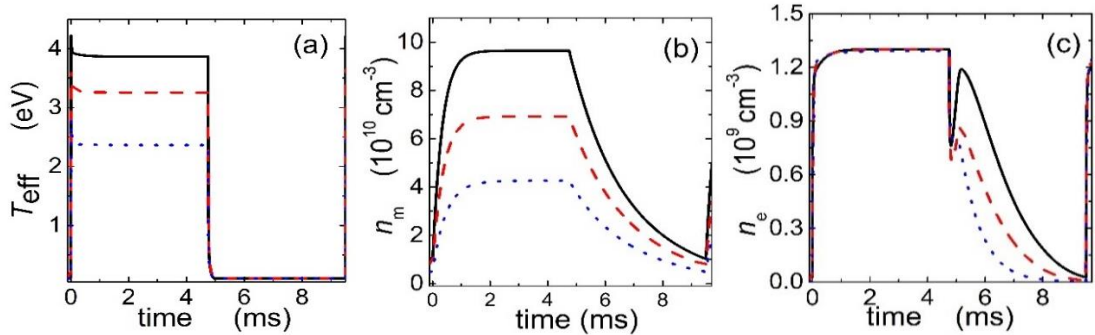


Fig. 2.  $T_{\text{eff}}$  (a),  $n_m$  (b) and  $n_e$  (c) in an argon/dust pulsed plasma for different  $x_F$ : 2 (solid line), 1.5 (dashed line) and 1.0 (dotted line). Here,  $n_e$  at the end of the on-period is  $1.3 \times 10^9 \text{ cm}^{-3}$ , as in Fig. 1(c).

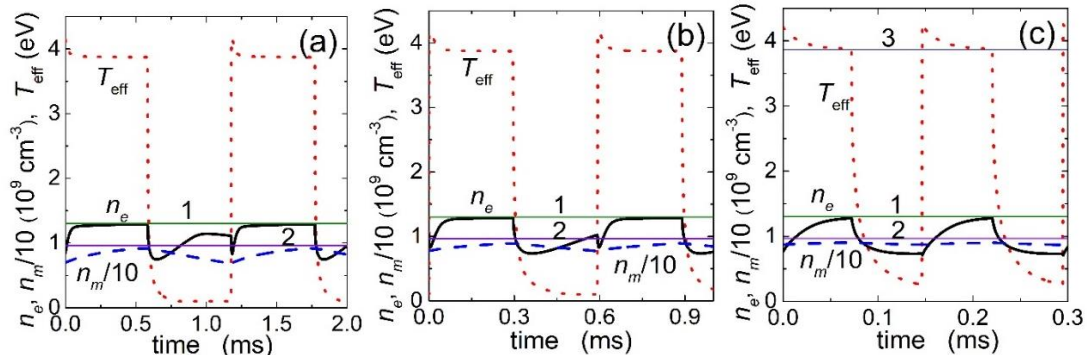


Fig. 3.  $n_e$  (solid line),  $n_m/10$  (dashed line) and  $T_{\text{eff}}$  (dotted line) as a function of time in Ar/dust pulsed plasma at  $x_F = 2$  and different  $v_p$ : 840 (a), 1680 (b) and 6720 (c) Hz. The line 1 describes  $n_e$ , the line 2 describes  $n_m/10$  and the line 3 (only in (c))  $T_{\text{eff}}$  for the CW plasma with  $P_{\text{abs}} = 12.6 \text{ W}$  (which equals to  $P_{\text{max}}$  in the pulsed plasma case).

Our model also shows that in the presence of dust and at some pulsing frequencies  $v_p$  the electron density decreases rapidly in the very beginning of the on-period (Fig. 3). In our opinion, this decrease is due to an enhancement of electron collection by dust particles at the beginning of the on-period. Further, variation in the pulsing frequency differently affects the metastable density in a dust-free and in a dusty plasma. For large pulsing frequencies ( $\geq 840$  Hz), the metastable density in presence of dust is smaller than in the continuous-wave (CW) discharge

(Fig. 3), contrary to the dust-free case [3]. In our opinion, this is due to faster variation of the effective electron temperature in the dusty case comparing with the  $n_d = 0$  case, because of collection of electrons by dust particles.

Using a 1D model for a dust-free Ar plasma afterglow, we also studied the charge of a dust particle and the forces affecting the dust particle as a function of time and spatial coordinate  $x$ . A plasma slab of  $L = 5$  cm size was considered. It was assumed that the spatial dependence for  $n_e$  is cosines-like,  $x_F = 2$ ,  $T_{\text{eff}}$  is spatially homogeneous and  $T_{\text{aft}} = 0.1$  eV. The calculations were carried out for  $a_d = 50$  nm,  $P = 0.1$  Torr and for the initial electron density in the slab midplane  $n_{e0} = 10^{10}$  cm<sup>-3</sup>. The electron temperature and density were obtained using the ambipolar diffusion approach, and the dust charge was calculated assuming that the ion current to a dust grain equals to that of electrons. The forces affecting the dust grain were calculated in the same manner as in [4].

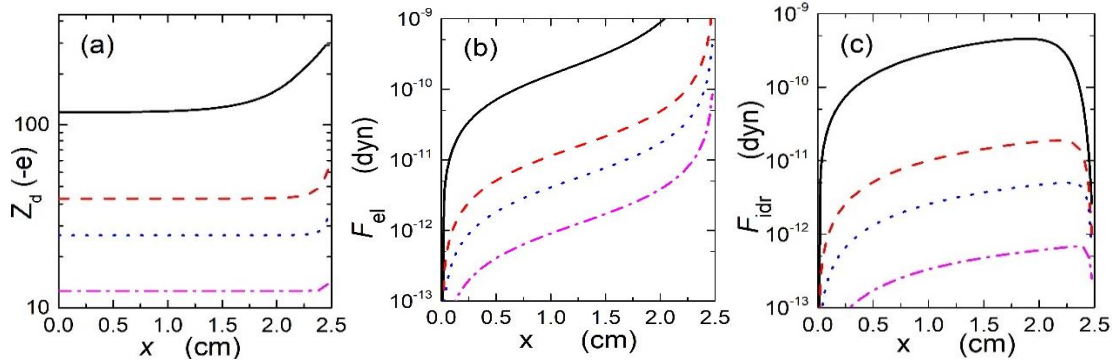


Fig.4. The spatial distributions of dust charge (a) and the electric (b) and ion drag forces affecting a dust grain in an afterglow plasma for  $t = 0$  (solid line),  $5 \times 10^{-2}$  ms (dashed line),  $0.1$  ms (dotted line) and  $0.3$  ms (dash-dotted line). Here,  $x=0$  and  $x=2.5$  cm correspond to the slab midplane and the slab boundary, respectively.

It was found that the amount of negative charge on the dust particle decreases rapidly in the beginning of the afterglow [Fig. 4(a)] because of decreasing the electron temperature, until  $T_{\text{eff}} = T_{\text{aft}}$ . The decrease is accompanied by decreasing the electron density and by a decrease of the electric and ion drag forces [Figs. 4(b) and 4(c)]. At large afterglow times (here,  $t \geq 0.3$  ms), the electron temperature becomes time-independent, and, as a result, the dust charge and the electric force are also nearly time-independent. In the late afterglow, the ion drag force is essentially smaller than the electric force [Figs. 4(b) and 4(c)] because of decreasing  $n_e$ .

- [1] Thorsteinsson E G and Gudmundsson J T 2009 *Plasma Sources Sci. Technol.* **18**, 045001
- [2] Stefanović I, Sadeghi N, Winter J and Sikimić B 2017 *Plasma Sources Sci. Technol.* **26**, 065014
- [3] Denysenko I B, Stefanović I, Mikikian M, Kovacevic E and Berndt J 2021 *J. Phys. D: Appl. Phys.* **54**, 065202
- [4] Schwabe M and Graves D B 2013 *Phys. Rev. E* **88**, 023101